

Electrochemical Corrosion Inhibition of Steel in Alkaline Chloride Solution

M.A. Ameer*, A.M. Fekry, A.A.Ghoneim, F.A. Attaby

Chemistry Department, Faculty of Science, Cairo University, Giza-12613, Egypt.

*E-mail: mameer_eg@yahoo.com

Received: 21 September 2010 / Accepted: 15 October 2010 / Published: 1 December 2010

Steel was polarized vs. saturated calomel electrode (SCE) in naturally aerated 1.0 M NaOH + 1.0M NaCl solutions (Blank) containing two organic inhibitors of different concentrations. The results of potentiodynamic polarization showed that corrosion current density, i_{corr} , decreases with increasing the concentration of organic inhibitors indicating a decrease in the corrosion rate as well as an increase in the inhibition efficiency of mild steel. Electrochemical impedance spectroscopy measurements and SEM confirmed well this behavior.

Keywords: EIS; mild steel, polarization, NaOH, NaCl, SEM

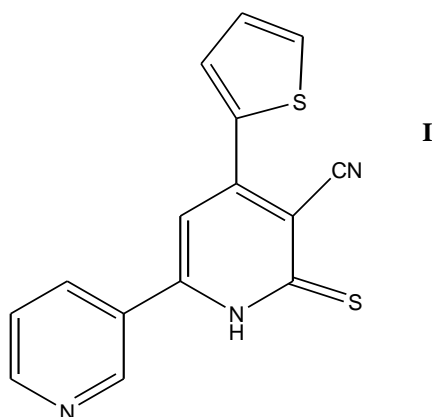
1. INTRODUCTION

The corrosion inhibition of steels has received a considerable amount of attention as a result of its industrial concern [1, 2]. Steel passivation in alkaline environments is due to the formation of a very thin, but highly protective oxide/hydroxide layer [3]. It has been proved that, in alkaline media, the film corresponds basically to a double-layer model consisting of an inner magnetite and an outer ferric oxide according to a $\text{Fe}_3\text{O}_4/\text{Fe}^{3+}$ structure [4–10]. The most internal layer is composed of Fe^{2+} oxides in contact with the substrate. The thermodynamic instability of both Fe^{2+} oxides and magnetite in the presence of oxygen leads to the formation of an outer layer of Fe^{3+} oxides and continuous exposure to oxygen and humidity promotes film growth and a progressive enrichment of the passive film in Fe^{3+} , either in oxide form or oxo-hydroxide form, depending on the potential. The passivity breakdown occurs by addition of Cl⁻ to the alkaline solution [11]. Most of the efficient inhibitors used in industry are organic compounds having multiple bonds in their molecules which mainly contain nitrogen and sulphur atoms through which they are adsorbed on the metal surface. Compounds with functional groups containing oxygen, nitrogen and sulphur have ability to form complexes with iron. They have

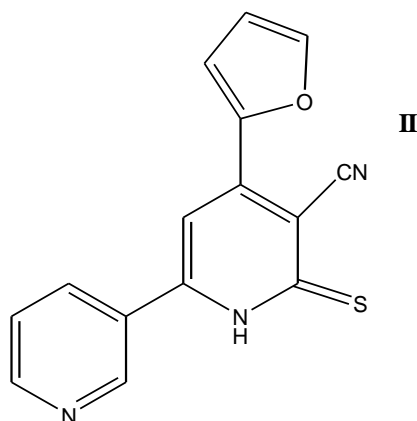
been reported to act as effective inhibitors to the surface of steel by means of their competitive adsorption through the surface complex formation. In practice corrosion can never be stopped but hindered to a reasonable level. Among many methods of corrosion control and prevention the organic inhibitors are the most frequently used [12]. Organic compounds used as inhibitors act through a process of surface adsorption, so the efficiency of an inhibitor depends on [13]:

- (i) the chemical structure of the organic compound,
- (ii) the surface charge of the metal, and
- (iii) the type of interactions between the organic molecule and metal surface.

Existing data reveal most inhibitors to act by adsorption on the metal surface through heteroatoms such as nitrogen, oxygen and sulphur, double bonds, triple bonds or aromatic rings which tend to form stronger coordination bonds. Compounds with π -bonds generally exhibit good inhibitive properties, the electrons for the surface interaction being provided by the π -orbital [13]. The main aim of this research work is to study the electrochemical behavior of reinforcement mild steel produced in Egypt for construction purposes, in different concentrations of organic inhibitors (newly synthesized heterocyclic compounds) [14] in blank solution. These compounds (Scheme 1) are required for several chemical transformations as well as our medicinal chemistry programs. Different techniques were employed such as potentiodynamic polarization and impedance spectroscopy (EIS).



1,2-dihydro-6-(pyridin-3-yl)-4-(thiophen-2-yl)-2-thioxopyridine-3-carbonitrile



4-(furan-2-yl)-1,2-dihydro-6-(pyridin-3-yl)-2-thioxopyridine-3-carbonitrile

Scheme 1.

2. MATERIALS AND METHODS

The steel rod was tested in the present study with its cross-sectional area of 0.4657 cm^2 . The composition of the steel is as follows (wt %): C = 0.31, Si = 0.21, Mn = 0.81, P = 0.014, S = 0.017, Cu = 0.06, Cr = 0.02, Mo = 0.01, Ni = 0.02, V = 0.002 and the balance is Fe. The test aqueous solutions contained 1.0 M NaOH + 1.0M NaCl (Aldrich) analytical reagent with pH = 12.3 (blank solution). Triple distilled water was used for preparing all solutions. In all measurements, abraded electrode was used. Polishing was affected using successively finer grade of emery papers (600-1200 grade). Polarization and electrochemical impedance spectroscopy (EIS) measurements were carried out using the electrochemical workstation IM6e Zahner-electrik GmbH, Meßtechnik, Kronach, Germany. The excitation AC signal had amplitude of 10 mV peak to peak in a frequency domain from 0.1 Hz to 100 kHz. The EIS was recorded after reading a steady state open-circuit potential. The scanning was carried out at a rate of 1 mV/s over the potential range from -1000 to 0 mV vs. saturated calomel electrode (SCE). Prior to the potential sweep, the electrode was left under open-circuit in the respective solution for ~ 1 hour until a steady free corrosion potential was recorded. Corrosion current, I_{corr} , which is equivalent to the corrosion rate is given by the intersection of the Tafel lines extrapolation. Because of the presence of a degree of nonlinearity in the Tafel slope part of the obtained polarization curves, the Tafel constants were calculated as a slope of the points after E_{corr} by ± 50 mV using a computer least-squares analysis. I_{corr} was determined by the intersection of the cathodic Tafel line with the open-circuit potential. For the steel over the concentration range studied, I_{corr} increases with increasing the molar concentration of the anion. All potentials were measured and given with respect to SCE ($E = 0.241$ V).

3. RESULTS AND DISCUSSION

3.1. EIS Measurements

3.1.1. Effect of inhibitor concentration

The EIS scans of mild steel alloy in dependence on the type and concentration of organic inhibitors were recorded after the working electrode was left in the test solution for 1 h to achieve its steady free corrosion potential (E_{st}) value with and without inhibitors. The experimental EIS are presented as Bode plots in Fig. 1(a-b). Fig.1c is an example of Nyquist plots of mild steel alloy in blank solution containing 1.0 mM of organic inhibitors I and II. The impedance ($|Z|$) of mild steel alloy is clearly found to depend on the inhibitor type and concentration. An increase in inhibitor concentration leads to an increase in the $|Z|$ value. The results in general, show two time constants, one of them has phase angle maximum $\sim 45^\circ$, corresponding to a diffusion control in the passive layer. The impedance data were thus simulated to the appropriate equivalent circuit (Fig.2). This simulation gave a reasonable fit with an average error of about 3%. The estimated data are given in Table 1. The appropriate equivalent model used to fit the high and low frequency data consists of two circuits in series from $R_{\text{ct}}\text{-}Z_{\text{w}}\text{-}CPE_{\text{d}}$ and $R_{\text{c}}\text{-}CPE_{\text{c}}$ parallel combination and the two are in series with R_{s} . In this

way CPE_d is related to contribution from the capacitance of the outer layer and the faradaic reaction therein and CPE_c pertains to the inner layer, while R_{ct} and R_c are the respective resistances of the outer and inner layers constituting the surface film, respectively [15].

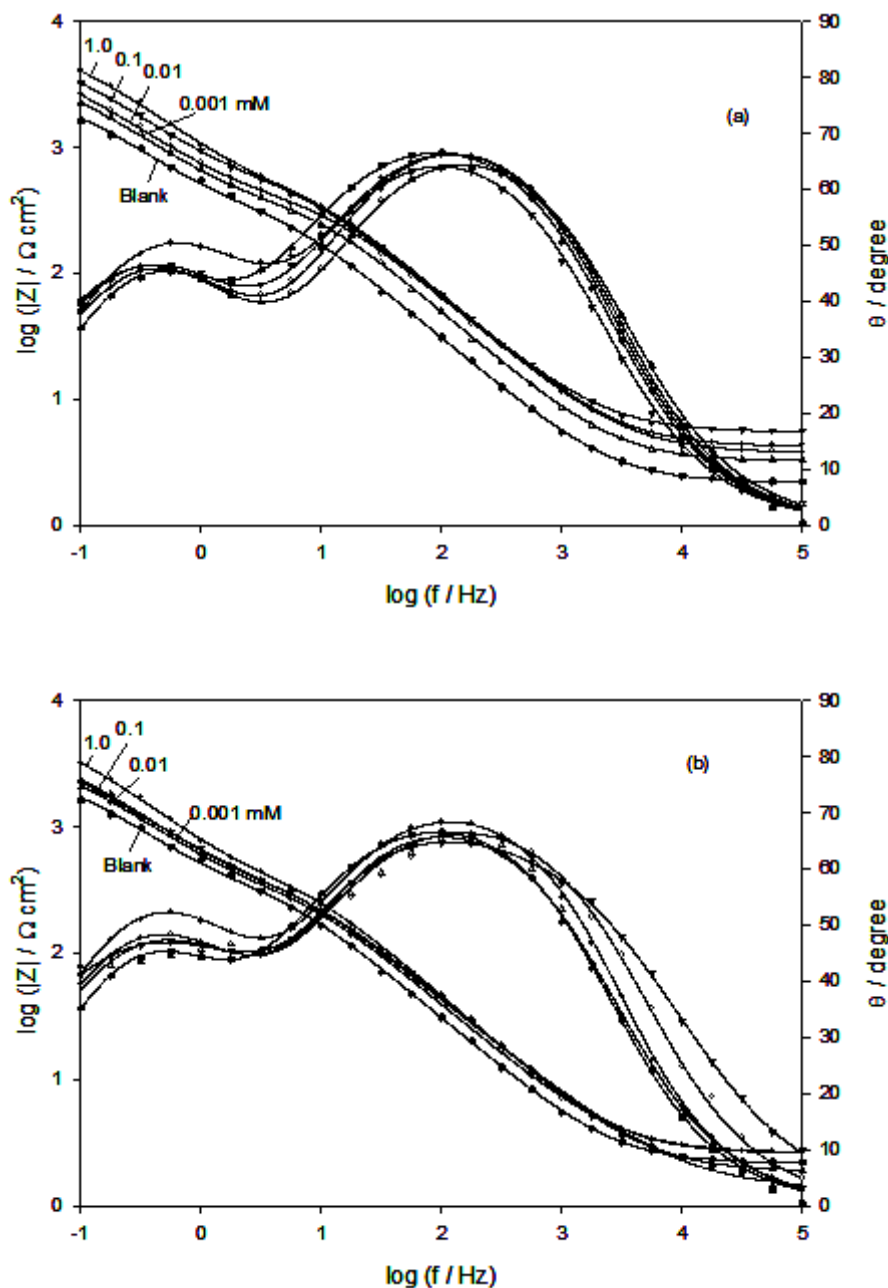


Figure 1. Bode plots of mild steel alloy in blank solution containing different concentrations of organic inhibitors: (a) I and (b) II

One of the peaks in Bode plots has phase angle maximum $\sim 45^\circ$, thereby an equivalent circuit with Warburg component Z_w might be more appropriate. A Warburg impedance (Z_w) can be linked to

ion diffusion through the passive film. Such diffusion process may indicate that the corrosion mechanism is controlled not only by a charge-transfer process but also by a diffusion process.

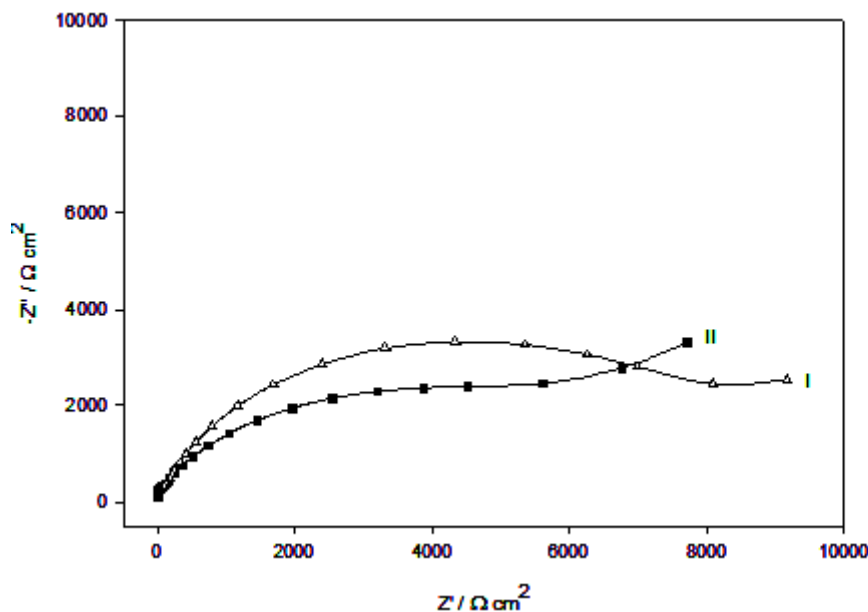


Figure 1.(c) Nyquist plots of mild steel alloy in blank solution containing 1.0 mM of organic inhibitors I and II.

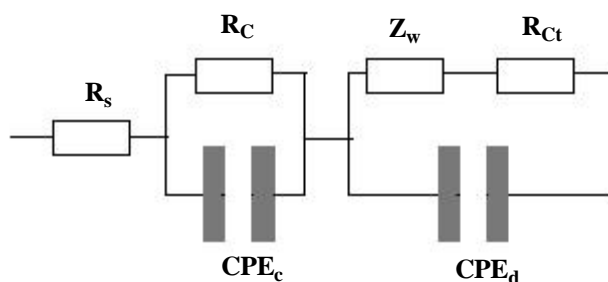


Figure 2. Equivalent circuit model representing two time constants.

Analysis of the experimental spectra were made by best fitting to the corresponding equivalent circuit using Thales software provided with the workstation where the dispersion formula suitable to each model was used [15]. In this complex formula an empirical exponent (α) varying between 0 and 1, is introduced to account for the deviation from the ideal capacitive behavior due to surface inhomogeneties, roughness factors and adsorption effects [16]. An ideal capacitor corresponds with $\alpha = 1$ while $\alpha = 0.5$ becomes the CPE in a Warburg component [17]. In all cases, good conformity between theoretical and experimental was obtained for the whole frequency range. Regarding the influence of concentrations of the two organic inhibitors on the total resistance of mild steel surface film, which is inversely proportional to the capacitance (C_T) of the film [18], Fig. 3 reveals generally concurrent features to the behavior of the film resistance. As given in Table 1, the resistance (R_T) and

the relative thickness ($1/C_T$) of the surface film on mild steel sample increase with increasing inhibitor concentration in blank solution and also the diffusion behavior increases.

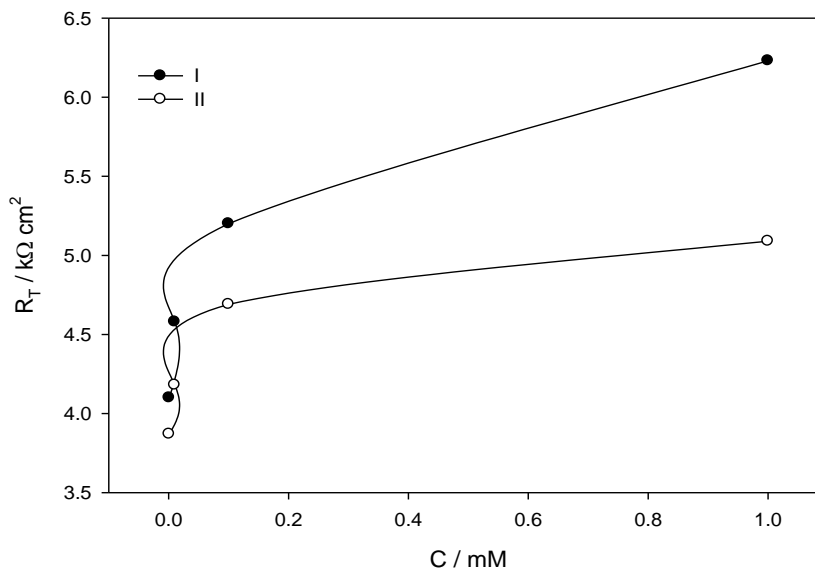


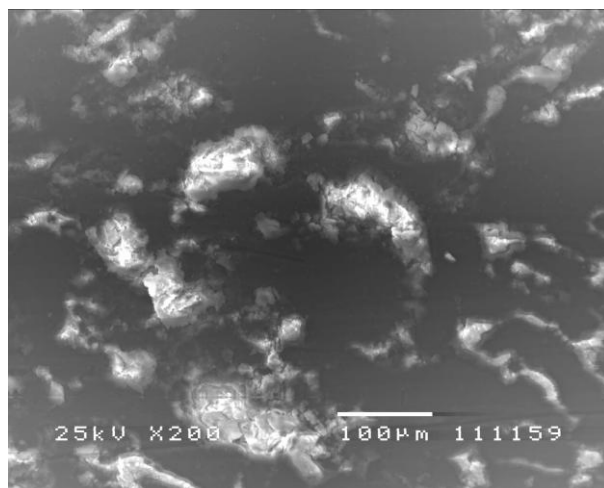
Figure 3. Variation of the total resistance (R_T) of mild steel in blank solution containing different concentrations of organic inhibitors.

Table 1. Impedance parameters for mild steel alloy in absence and presence for organic inhibitors of different concentrations, at 298 K

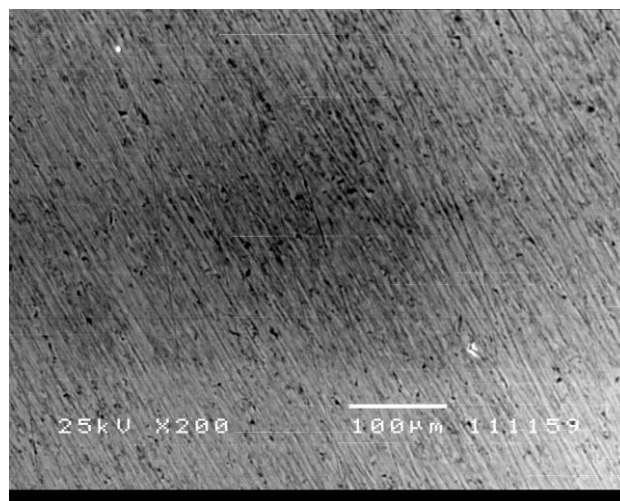
Inh. No.	C mM	R_s Ω cm ²	R_{ct} kΩ cm ²	CPE_d μF cm ⁻²	α_d	R_c kΩ cm ²	CPE_c μF cm ⁻²	α_c	W kΩ cm ² s ^{-1/2}	R_T kΩ cm ²	$1/C_T$ μF ⁻¹ cm ²	%IE
I	0.00	3.4	0.13	164.8	0.70	0.81	159.3	0.83	0.86	0.94	0.012	0.00
	0.001	1.7	0.96	97.40	0.76	3.14	80.2	0.87	1.08	4.10	0.023	77.1
	0.010	1.6	0.98	93.60	0.76	3.60	68.9	0.83	1.23	4.58	0.025	79.5
	0.100	1.5	1.04	93.30	0.79	4.16	62.8	0.86	1.44	5.20	0.027	81.9
	1.000	2.1	1.11	91.40	0.68	5.12	55.3	0.89	1.65	6.23	0.029	84.9
II	0.00	3.4	0.13	164.8	0.65	0.81	159.3	0.83	0.86	0.94	0.012	0.00
	0.001	1.6	0.78	102.00	0.75	3.09	84.8	0.84	0.94	3.87	0.022	75.7
	0.010	1.2	0.84	98.60	0.75	3.34	70.1	0.86	0.99	4.18	0.024	77.5
	0.100	1.6	0.91	95.70	0.74	3.78	66.7	0.84	1.04	4.69	0.025	80.0
	1.000	2.3	0.94	93.10	0.77	4.15	64.6	0.86	1.31	5.09	0.026	81.5

Thus, when inhibitor concentration increases, more inhibitor molecules will be adsorbed on the surface through the active centers in each compound. As shown in Table 1, R_T value of the two inhibitors is higher than that of the blank and is in the following order $I > II > \text{blank}$. This order may be due to the active centers in each compound. Thus, it was found that compound I has the highest total

resistance value due to it has the most electron rich environment that can be adsorbed well on the steel surface.



(a)



(b)

Figure 4. SEM graphs for the steel in:(a) 1.0 M NaOH with 1.0 M Cl^- (blank); (b) blank + 1.0 mM of compound I.

Such action could be explained through the lone pair of S of thiophene in compound I which are freely liberated into the system than O of furan in compound II. Also the O atom of compound II is much more restricted to liberate its electrons than S atom in compound I. Thus, the transition of metal/solution interface from a state of active dissolution for the blank to the passive state by adding the inhibitor is attributed to the adsorption of the inhibitor molecules on the metal surface, forming a protective film. This behavior is confirmed by SEM micrographs, as shown in Fig. 4 for: (a) blank (1.0 M NaOH + 1.0M NaCl) and (b) blank + 1.0 mM organic inhibitor I (inhibited). It shows a denser and

smoother film adsorbed on the alloy surface for inhibited mild steel than that for the blank. The rate of adsorption is usually rapid and hence, the reactive metal surface is shielded from the aggressive environment [19].

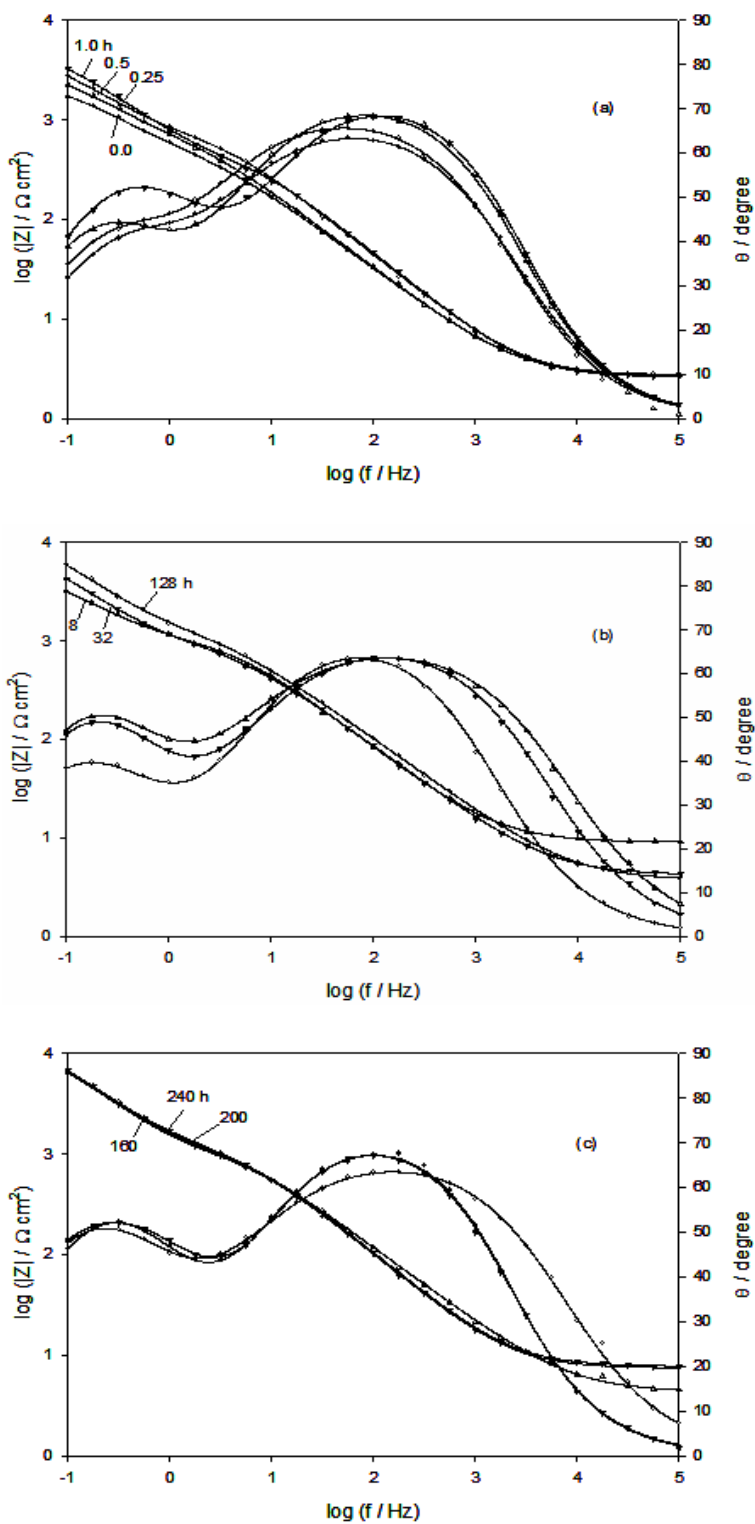


Figure 5. Bode plots of mild steel alloy in blank solution containing 1.0 mM of organic inhibitor I with immersion time.

3.1.2. Effect of immersion time

EIS is a useful technique for long time tests, because they don't significantly disturb the system and it is possible to follow it over time. The present work was carried out in **blank solution** containing 1.0 mM of compound (I) for 240 h. Fig.5(a-c) represent Bode plots of mild steel alloy in blank solution containing 1.0 mM of organic inhibitor I with time of immersion. From EIS data, it is obvious that both R_T and $1/C_T$ values increased sharply during the initial 3h and remained fairly constant afterward, Fig.6.

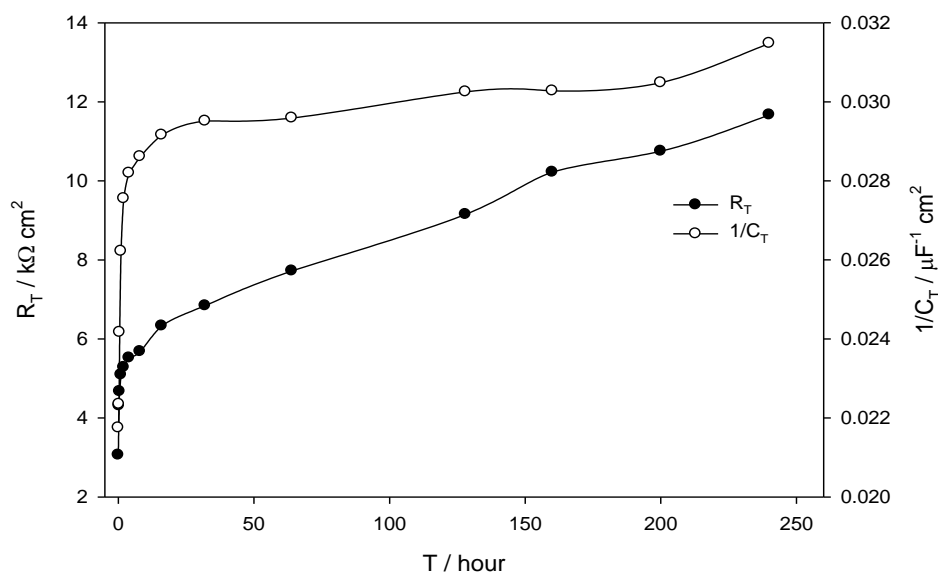


Figure 6. Variation of the total resistance (R_T) and the relative thickness ($1/C_T$) of mild steel alloy in blank solution containing 1.0 mM of organic inhibitor I with time of immersion, at 298 K.

This means that the formation of the inhibitor surface film, and therefore the inhibitor adsorption, on the electrode surface was fast and completed within 3h. This is consistent with the adsorption effect of inhibitor and steel corrosion products to increase the protective power of the passive film and a compact adsorbed film of the inhibitor is formed on the steel surface [16]. Competitive adsorption is assumed to occur on the steel surface between the aggressive OH^- ions and the anions of the inhibitor molecule [17].

3.2. Potentiodynamic Polarization Measurements

3.2.1. Effect of inhibitor concentration

In this part the potentiodynamic polarization behavior of steel was studied in relation to inhibitor type and concentration. The potential was scanned automatically from -1.0 to 0.0 V vs. SCE at a rate of 1 mV s^{-1} which allows the quasi-stationary state measurements. Prior to the potential scan

the electrode was left under open circuit conditions in the respective solution for 1 h until a steady free corrosion potential (E_{st}) value was recorded.

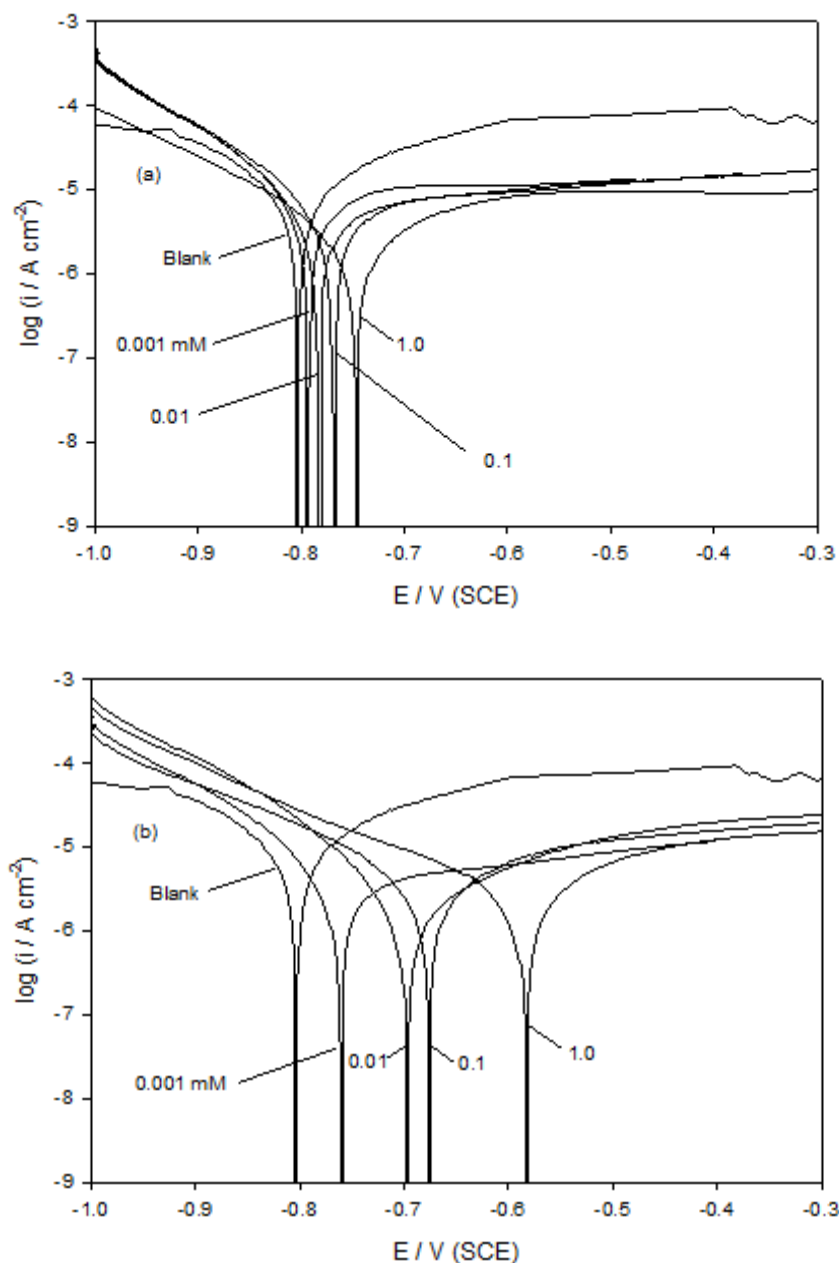


Figure 7. Potentiodynamic polarization scans of mild steel alloy in blank solution containing different concentrations of organic inhibitors (a) I and (b) II, at 298 K.

Fig. 7(a,b) shows linear sweep potentiodynamic traces for the steel in blank solution containing different concentrations of I, II organic inhibitors, respectively. It is noticed that the corrosion potential shifts towards more positive potential as the inhibitor concentration increases, indicating that these inhibitors promote passivation of iron through adsorption. These results enable the determination of various electrochemical corrosion parameters of the electrode using Thales software for i/E analysis.

The corrosion current was determined by the intersection of the cathodic or the anodic Tafel line with the OCP (potential of zero current in the potentiodynamic curves or E_{corr}).

Table 2. Impedance parameters for mild steel alloy for organic inhibitor I of 1.0 mM concentration in blank with immersion time, at 298 K

Time	R_s	R_{ct}	CPE_d	α_d	R_c	CPE_c	α_c	W	R_T	$1/C_T$
hour	$\Omega \text{ cm}^2$	$\text{k}\Omega \text{ cm}^2$	$\mu\text{F cm}^{-2}$		$\text{k}\Omega \text{ cm}^2$	$\mu\text{F cm}^{-2}$		$\text{k}\Omega \text{ cm}^2 \text{ s}^{-1/2}$	$\text{k}\Omega \text{ cm}^2$	$\mu\text{F}^{-1} \text{ cm}^2$
0.00	2.5	0.75	95.00	0.75	2.31	89.1	0.79	0.68	3.06	0.022
0.25	2.4	0.79	93.90	0.76	3.52	85.5	0.80	0.81	4.31	0.023
0.50	2.3	0.86	93.70	0.68	3.81	74.1	0.89	0.94	4.67	0.024
1.00	2.3	0.94	91.10	0.79	4.15	64.6	0.82	1.31	5.09	0.027
2.00	2.3	0.94	91.40	0.77	4.34	60.2	0.86	1.35	5.28	0.028
4.00	2.3	0.96	90.80	0.78	4.56	58.2	0.81	1.75	5.52	0.028
8.00	2.3	0.97	89.60	0.82	4.71	57.3	0.77	1.78	5.68	0.029
16.00	2.3	1.01	87.50	0.83	5.32	56.4	0.75	1.79	6.33	0.029
32.00	2.3	1.04	87.50	0.83	5.80	55.3	0.84	1.93	6.84	0.030
64.00	2.2	1.32	87.40	0.80	6.40	55.1	0.75	1.96	7.72	0.030
128.00	2.8	1.65	87.30	0.77	7.50	53.2	0.87	1.99	9.15	0.030
160.00	2.2	2.12	87.10	0.75	8.10	53.2	0.79	2.30	10.22	0.030
200.00	2.3	2.25	86.90	0.76	8.50	52.7	0.80	2.30	10.75	0.031
240.00	2.5	2.87	86.80	0.68	8.80	50.1	0.89	2.34	11.67	0.032

This point determines the potential (E_{corr}) and current density (i_{corr}) for corrosion. For all tested concentrations, the active dissolution parameters including the values of the corrosion potential (E_{corr}) and corrosion current density (i_{corr}) are given in Table 3 for both uninhibited and inhibited mild steel. The inhibition efficiency (IE %) are also given in Table 3 and calculated from the following equation:

$$\text{IE}\% = 1 - \frac{i_{\text{inh}}}{i_{\text{corr}}} \times 100 \quad (1)$$

where i_{corr} and i_{inh} are the uninhibited and inhibited corrosion current densities, respectively.

It was found that the inhibition efficiency for compound I (1.0 mM) is 67.26 % which is the higher inhibition efficiency. Furthermore, it can be seen that usually when the concentration of compounds I, II increased, the inhibition efficiencies (IE) increased reaching their maximum value, 92.45 % and 80.50 at 1.0 mM for compound I and II, respectively, at 298 K as shown in Fig.8.

It can be seen from the experimental results derived from polarization curves that increasing organic inhibitor concentration decreased i_{corr} significantly at all of the studied concentrations. For compounds I&II, a positive shift in corrosion potential was observed (Fig. 7a,b). The shift in corrosion

potential towards the anodic side indicates that compounds I&II are an efficient anodic inhibitor for mild in blank solution. The increase in efficiency may be due to the blocking effect of the surface by both adsorption and film formation mechanism which decreases the effective area of attack. Results of the inhibition efficiencies revealed the good inhibiting action of inhibitors at high concentrations. The decrease of the corresponding current densities with increasing the inhibitor concentration was the consequence of the inhibitor adsorption on the steel surface. The higher IE exhibited by the compound may be attributed to its adsorption on the metal surface through polar groups (S or O) as well as through π -electrons of the double bond. This leads to greater coverage of the metal surface by the compound, thereby resulting in higher IE.

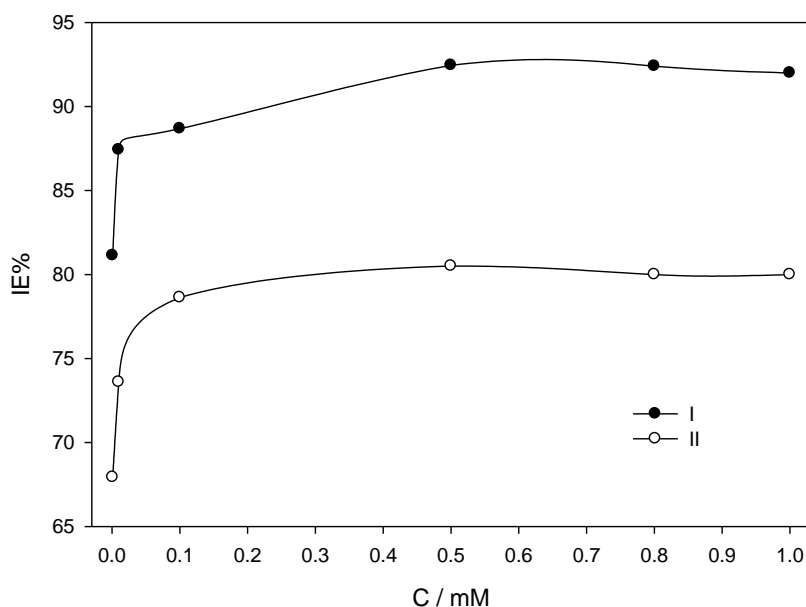


Figure 8. Variation of IE% for mild steel alloy in blank solution containing different concentrations of organic inhibitors, at 298 K.

3.3. Adsorption isotherm

Concerning the effectiveness of an organic inhibitor, it has been found that high corrosion inhibition performance depends on some key parameters as the nature and chemical structure of the inhibitor, as well as the type of the electrolyte [18]. It shows that the presence of low concentrations from the inhibitor in the corroding medium sharply decreases the dissolution rate of the alloy. Beyond this range, a rather abrupt change occurs such that inhibition reaches nearly a plateau over which an increase in inhibitor concentration has little effect on the corrosion rate and, consequently, on the percent inhibition. All these factors are mainly responsible for the formation of an adsorbed protective film. The surface coverage θ was calculated from the following equation:

$$\theta = 1 - \frac{i_{inh}}{i_{corr}} \quad (2)$$

Data obtained from polarization measurements were tested graphically for fitting various isotherms including Langmuir, Frumkin and Temkin. By far for this compound gives the best fit with Langmuir isotherm (Fig. 9). According to this isotherm θ is related to inhibitor concentration. The degree of surface coverage (θ) for different concentrations of inhibitor in blank has been evaluated and found to increase with increasing the concentration of additive.

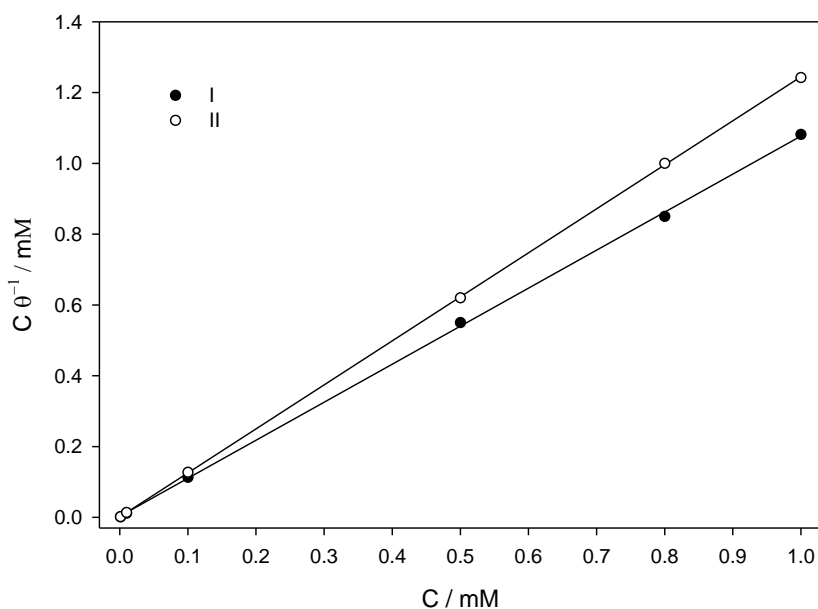


Figure 9. Langmuir isotherm adsorption model on the steel surface in blank solution containing different concentrations of organic inhibitors, at 298 K.

With regard to Langmuir adsorption isotherm according to the following equation:

$$\frac{C}{\theta} = \frac{1}{K_{ads}} + C \quad (3)$$

K_{ads} is the adsorption-desorption equilibrium constant. By plotting C/θ versus C at 298 K, straight line is obtained as seen in Fig.8. From the intercept, K_{ads} value was calculated for the adsorption process and found to be 0.847×10^3 , $0.35 \times 10^3 \text{ M}^{-1}$ for compounds I and II, respectively. However, the slope of the relation shows a little deviation from unity, this might be the result from the interactions between the adsorbed species on the metal surface [20, 21]. The K_{ads} value may be taken as a measure of the strength of the adsorption forces between the inhibitor molecules and the metal surface [22]. It was found that K_{ads} value is in the order $I > II$, thus, compound I has the higher value

(better one). The adsorption equilibrium constant, K_{ads} , is related to the standard free energy, ΔG_{ads}° , with the following equation:

$$\log K_{ads} = \log \frac{1}{55.5} + \frac{\Delta G_{ads}^{\circ}}{2.303 RT} \quad (4)$$

The values of ΔG_{ads}° at 298K are $-26.66 \text{ kJ mol}^{-1}$ and $-24.47 \text{ kJ mol}^{-1}$ for steel in blank with compound (I) and (II), respectively indicating that in blank solution the two compounds adsorb on steel surface via a physisorption-based mechanism[23].

Table 3. Corrosion parameters for mild steel alloy in absence and in presence of different concentrations organic inhibitors at 298 K

Inhibitor	C	i_{corr}	$-E_{corr}$	$-E_{passive}$	$-E_{flade}$	i_{crit}	% IE
No.	mM	$\mu\text{A cm}^{-2}$	mV(SCE)	mV(SCE)	mV(SCE)	$\mu\text{A cm}^{-2}$	
I	0.00	1.59	803.2	0.58	0.75	19.95	-
	0.001	0.30	794.7	0.57	0.74	7.94	81.13
	0.010	0.20	782.7	0.56	0.73	5.37	87.42
	0.100	0.18	767.4	0.56	0.72	4.46	88.68
	1.000	0.12	748.2	0.55	0.71	2.88	92.45
II	0.00	1.59	803.2	0.58	0.75	19.95	-
	0.001	0.51	760.5	0.63	0.73	5.24	67.93
	0.010	0.42	678.2	0.55	0.72	3.23	73.59
	0.100	0.34	699.5	0.53	0.64	2.95	78.62
	1.000	0.31	582.3	0.49	0.52	2.51	80.50

4. CONCLUSIONS

- i- The results showed that R_T value increases with increasing inhibitor concentration indicating a decrease in corrosion rate of the steel. Also, R_T value increases in the order $I > II$ for the two newly used organic inhibitors.
- ii- The corrosion rate (i_{corr}) increases with decreasing the inhibitor concentration.
- iii- EIS measurements under open circuit conditions confirmed well polarization results.
- iv- compound I has shown very good inhibition efficiency (IE) in blank solutions reaches to 98.74 % for 1.0 mM concentration.

References

1. E. Sarmiento, J. G. González-Rodríguez, J. Uruchurtu, O.Sarmiento, M. Menchaca, *Int. J. Electrochem. Sci.*, 4(2009)134.
2. Yanyan Yang, Lifan Xiao, Yanqiang Zhao and Fengyun Wang, *Int. J. Electrochem. Sci.*, 3(2008)56.
3. L. Freire, X.R. Nóvoaa, M.F. Montemor, M.J. Carnezimb, *Mat. Chem. and Phy.* 114 (2009) 962.
4. M. Nagayama, M. Cohen, *J. Electrochem. Soc.* 109 (1962) 781.
5. D. Rahner, *Sol. State Ionics* 86–88 (1996) 865.
6. D.D. Macdonald, *Pure Appl. Chem.* 71 (1999) 951.
7. B. Macdugall, M.J. Graham, Growth and stability of passive films, in: P. Marcus, J. Oudars (Eds.), *Corrosion Mechanisms in Theory and Practice*, Marcee Decker Pub., NY, 1995, p. 143.
8. S. Joiret, M. Keddama, X.R. Nóvoa, M.C. Pérez, C. Rangel, H. Takenouti, *Cem. Concr. Compos.* 24 (2002) 7.
9. A.J. Davenport, L.J. Oblonsky, M.P. Ryan, M.F. Toney, *J. Electrochem. Soc.* 147 (2000) 2162.
10. D. D. N. Singh, Rita Ghosh, B. K. Singh, *Corrosion Sci.* 44 (2002) 1713.
11. K. Yazdanfar, X. Zhang, P.G. Keech, D.W. Shoesmith, J.C. Wren, *Corrosion Sci.* 52(2010) 1297.
12. S.M. Abd El Haleem, S. Abd El Wanees, E.E. Abd El Aal, A. Diab, *Corrosion Sci.* 52 (2010) 292.
13. Ü. Ergun, D. Yüzer, K.C. Emregül, *Mat. Chem. and Phy* 109 (2008) 492.
14. A.Abdel-Fattah , M.Elneairy , M.Gouda , F.Attaby, Phosphorus, Sulfur, Silicon and other related Elements. 183(2008) 1592 .
15. M.A.Ameer, A.M.Fekry, A.A.Ghoneim, *Corrosion* 65 (2009) 587.
16. M.A. Ameer, A.A. Ghoneim, F. Heakal, A.M. Fekry, *Surf. Interface Anal.* 42(2010) 4 95.
17. U. Retter, A. Widmann, K. Siegler, H. Kahlert, *J. Electroanal. Chem.* 546 (2003) 87.
18. M. Montemor, A. Simões, M. Ferreira, M. Da Cunha, *Corros. Sci.* 41 (1999) 17.
19. A.M. Fekry , A.A. Gasser , M.A. Ameer, *Appl. Electrochem.* 40(2010) 739.
20. A.Azim, L.A. Shalaby, H. Abbas, *Corros. Sci.* 14 (1974) 21.
21. M.A. Migahed, H.M. Mohamed, A.M. Al-Sabagh, *Mater. Chem. Phys.* 80 (2003) 169.
22. M.A.Amin, *Applied Electrochem.* 36(2006)215.
23. E. Stupnišek-Lisac, A. Gazivoda, M. Madžarac, *Electrochim. Acta.* 47 (2002) 4189.